

Supporting information

Performance improvement of resistive switching memory achieved by reducing the size of MoS₂ embedded in poly(vinyl alcohol) films

Zipan Jiao^a, Xinglan Zhou^a, Junjie Yu^a, Xiaoyan Lan^a, Yi Shi^b, Jitong Li^a, Bingxin Liu^a,
Yongcheng Li^a, Guilin Chen^c, Rimeng Hu^d, Peng Zhang^{a,*} and Benhua Xu^{b,*}

^a School of Mechanical Engineering, Qinghai University, Xining 810016, P. R. China.

^b Chemical Engineering College, Qinghai University, Xining 810016, P. R. China.

^c Zhejiang Hikstor Technology Company Ltd., Hangzhou 311300, Zhejiang, China.

^d Institute for Advanced Interdisciplinary Research (iAIR), School of Chemistry and Chemical Engineering, Institute for Smart Materials & Engineering, University of Jinan, Jinan, 250022, P.R. China

*Correspondence: zhangpeng@qhu.edu.cn (P. Zhang); xubenhua@qhu.edu.cn (B. H. Xu)

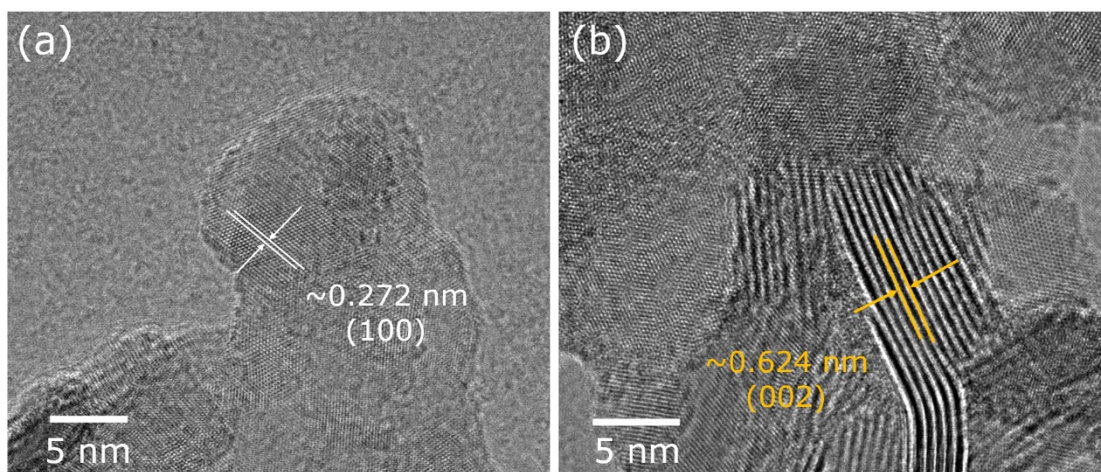


Fig. S1 High-resolution transmission electron microscopy (HRTEM) images of MoS₂ nanosheets.

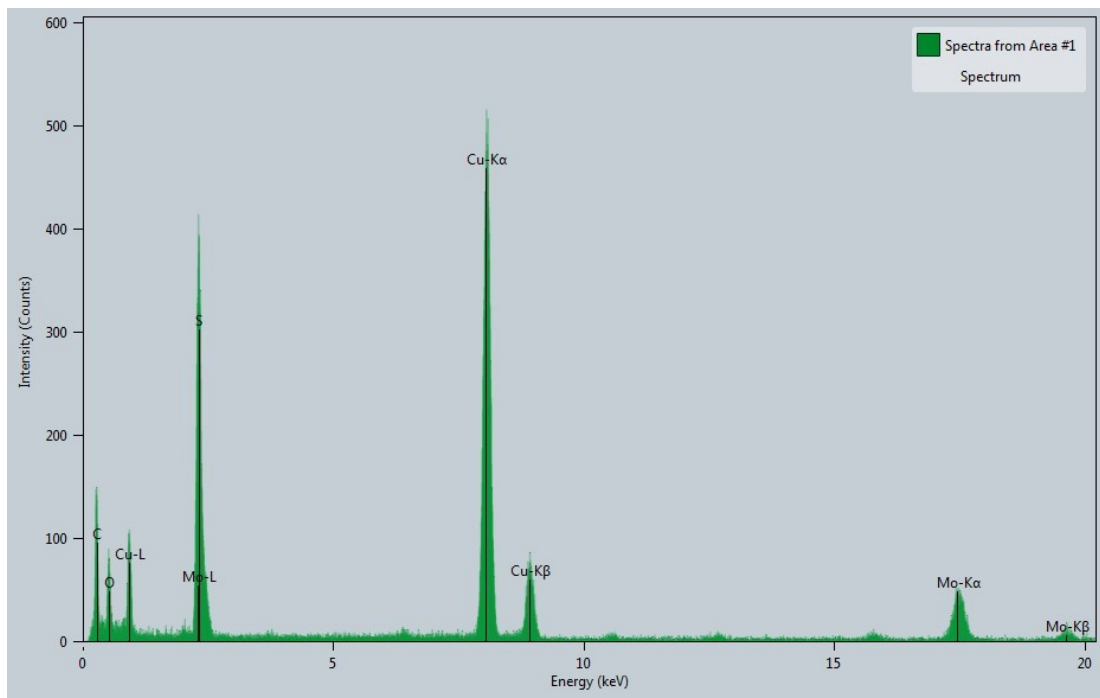


Fig. S2 EDS mapping of elemental content of MoS_2 nanosheets.

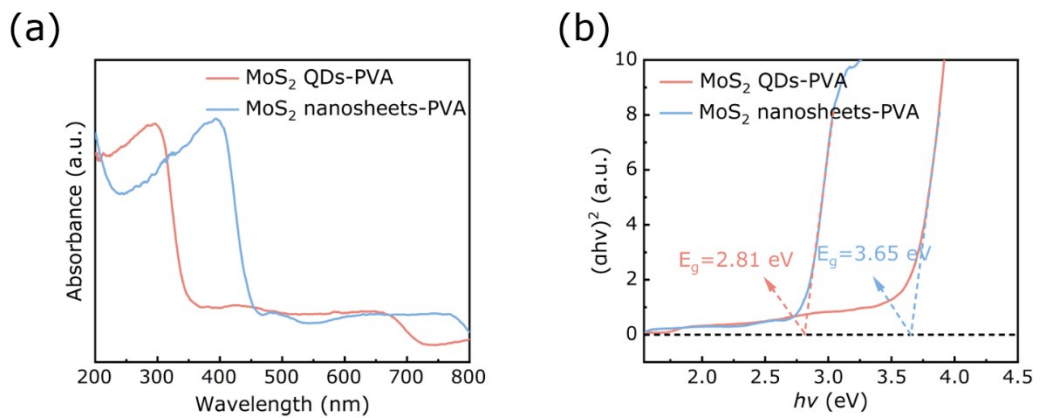


Fig. S3 (a) The UV-vis spectra and (b) corresponding Tauc plots of MoS₂ nanosheets-PVA films and MoS₂ QDs-PVA films.

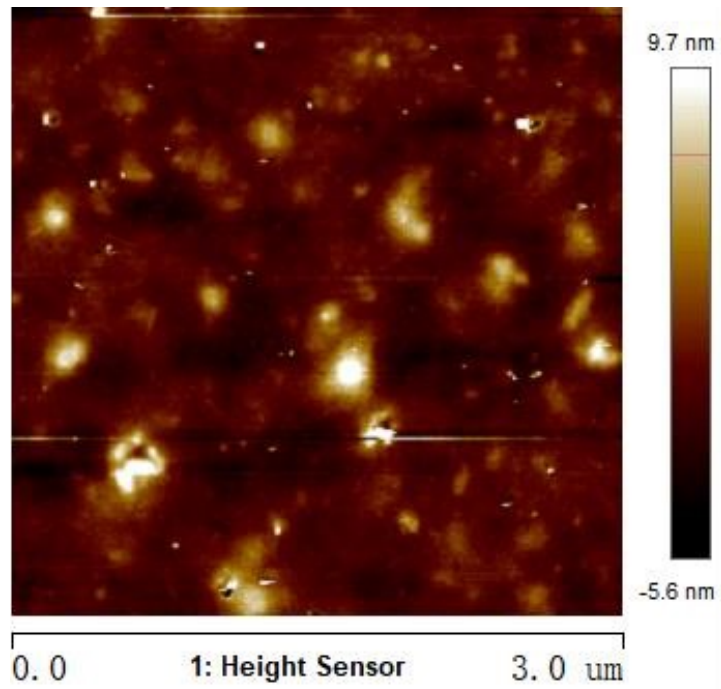


Fig. S4 AFM map of MoS₂ QDs-PVA hybrid thin film surface.

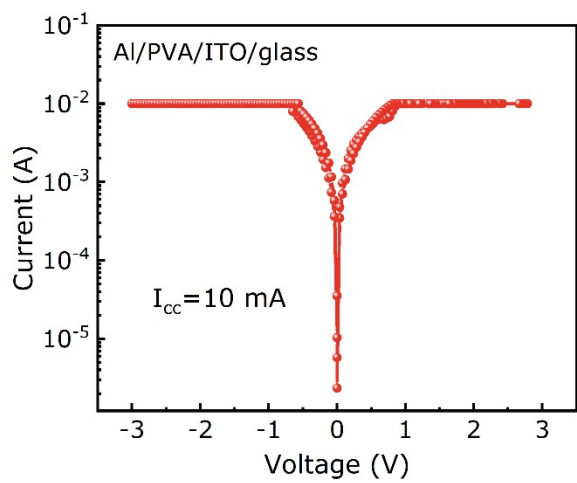


Fig. S5 The I-V diagram of Al/PVA/ITO/glass device.

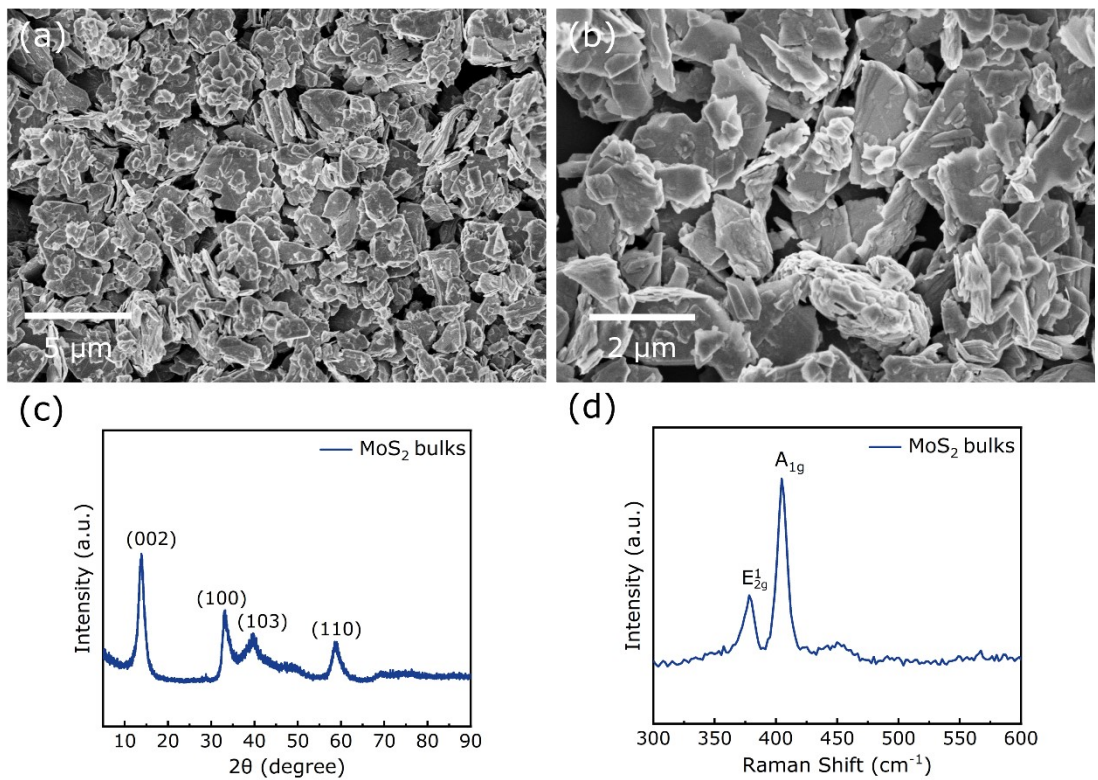


Fig. S6. (a-b) SEM image, (c) XRD pattern and (d) Raman pattern of MoS_2 bulks.

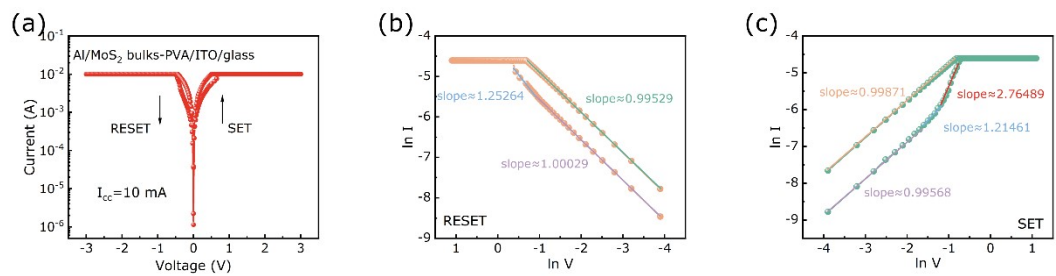


Fig. S7 (a) The I-V curves and (b-c) double logarithmic curves of Al/MoS₂ bulks-PVA/ITO/glass devices.

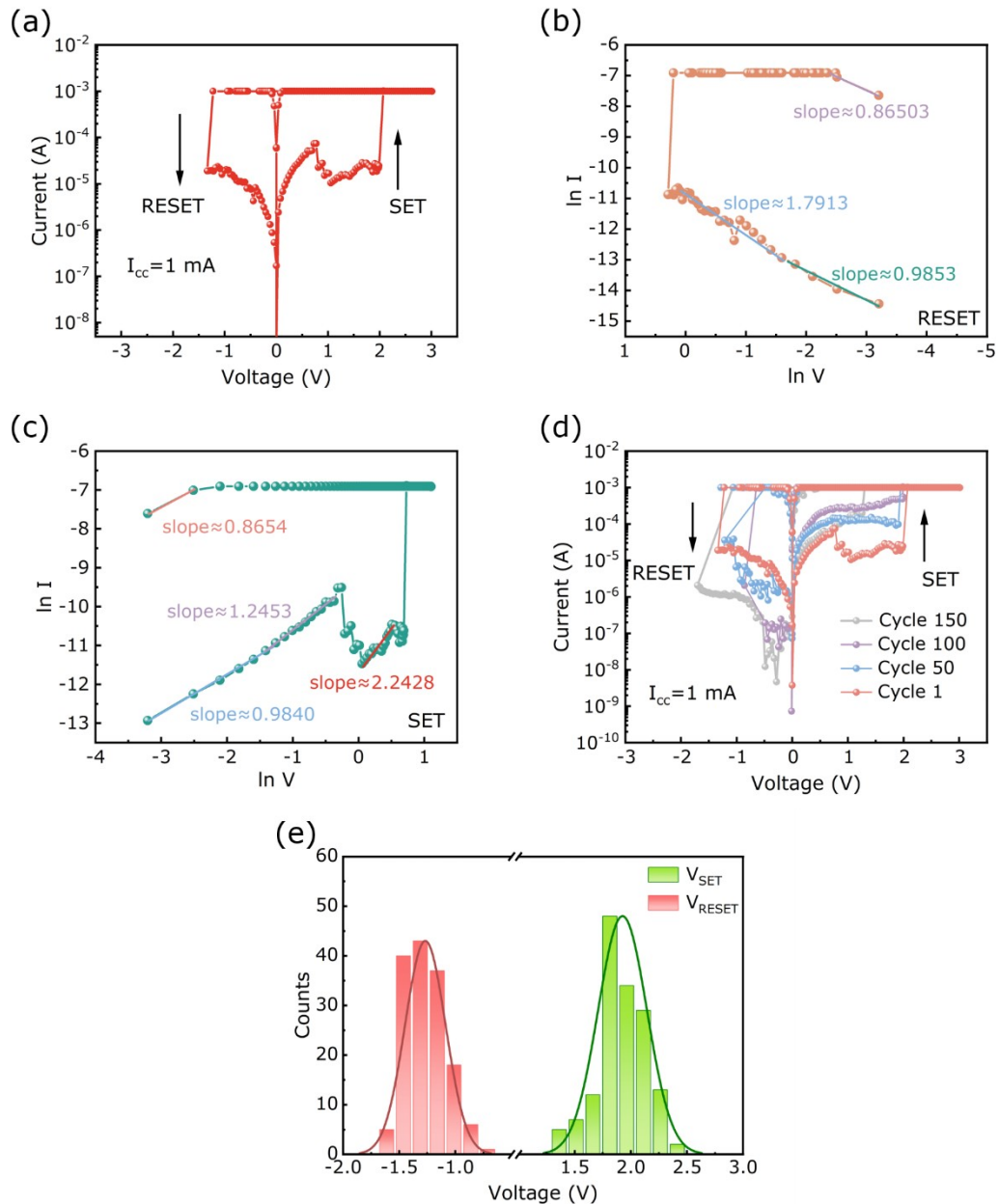


Fig. S8 (a) The I-V curves, (b-c) double logarithmic curves during SET and RESET processes, (d) I-V curves for 150 cycles, and (e) histograms of the distribution of V_{SET} and V_{RESET} for the Al/MoS₂ QDs-PVA/ITO/glass device at a compliance current of 1 mA.

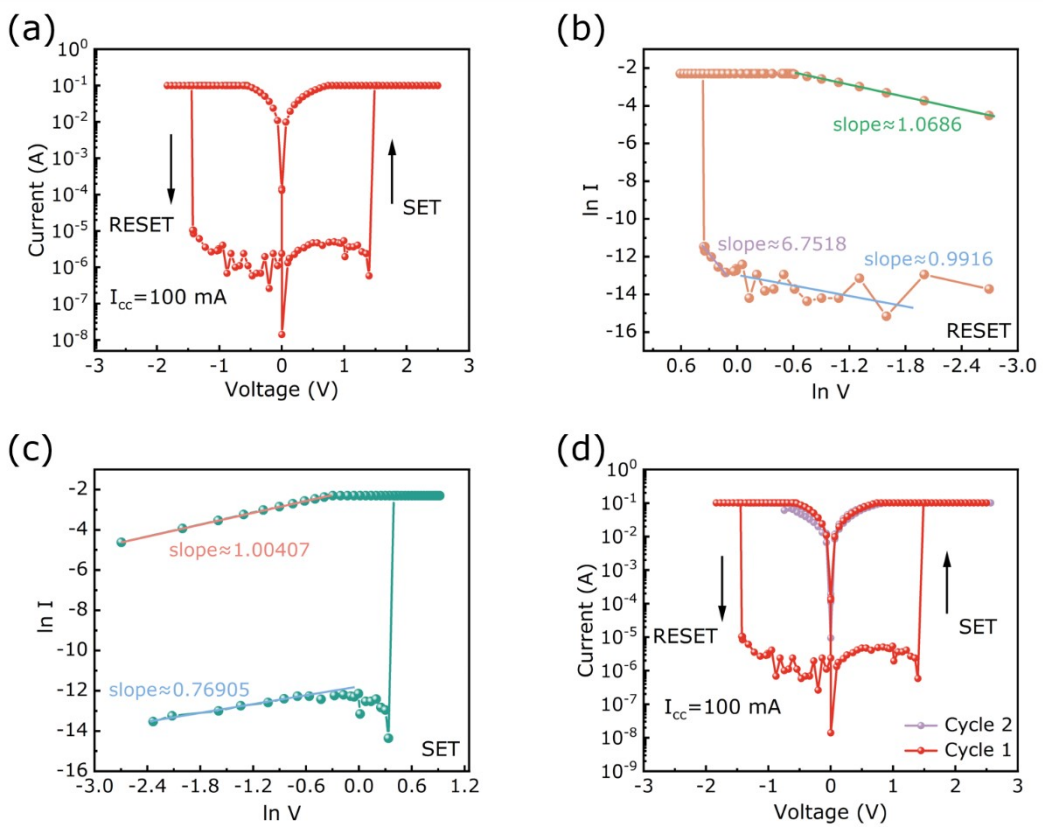


Fig. S9 (a) The I-V curves, (b-c) double logarithmic curves during SET and RESET processes, and (d) I-V curves for 2 cycles for the Al/MoS₂ QDs-PVA/ITO/glass device at a compliance current of 100 mA.

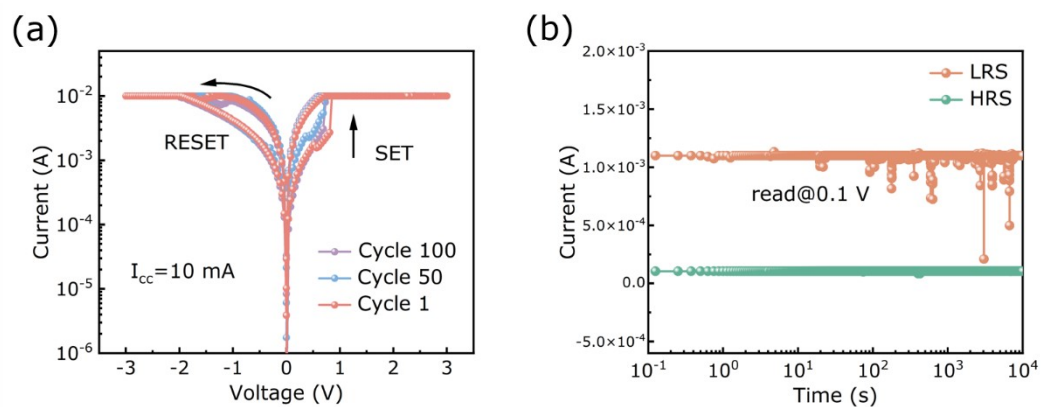


Fig. S10 (a) I-V curves for 100 cycles and (b) I-t plot for Al/MoS₂ nanosheets-PVA/ITO/glass device.

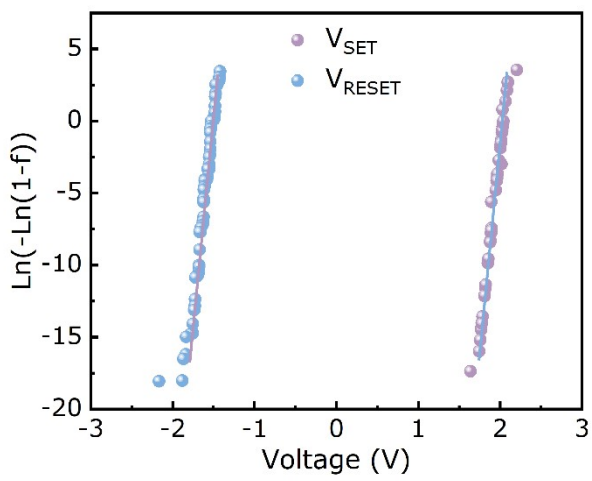


Fig. S11 Weibull distribution of V_{SET} and V_{RESET} for Al/MoS₂ QDs-PVA/ITO/glass device.

Table S1 Statistical measures and Weibull distribution parameters of Al/MoS₂ QDs-PVA/ITO/glass devices.

Parameters	Mean (V)	Standard deviation (V)	Coefficient of variation	β	x _{63%}
V _{SET}	1.98097	0.16951	0.08557	101.6030	2.04
V _{RESET}	-1.56886	0.14833	0.09455	81.4538	1.619

The Weibull cumulative distribution function for V_{SET} and V_{RESET} is defined as
11,12:

$$f = 1 - \exp[-(\frac{|V|}{\alpha})^\beta]$$

where α is the scale parameter of the Weibull distribution at 63.2% and β is the shape/slope parameter, which measures the spread of the distribution.

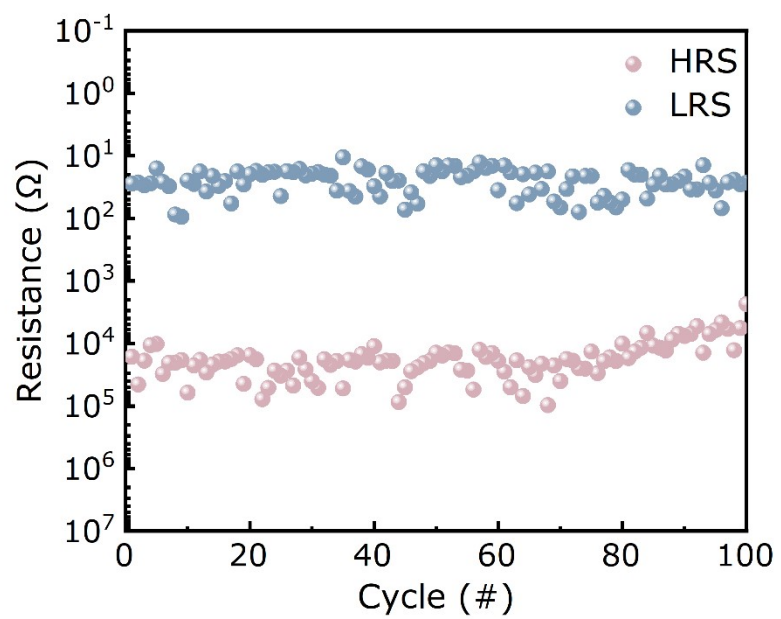


Fig. S12 Resistance variation of Al/MoS₂ QDs-PVA/ITO/glass device for 100 cycles.

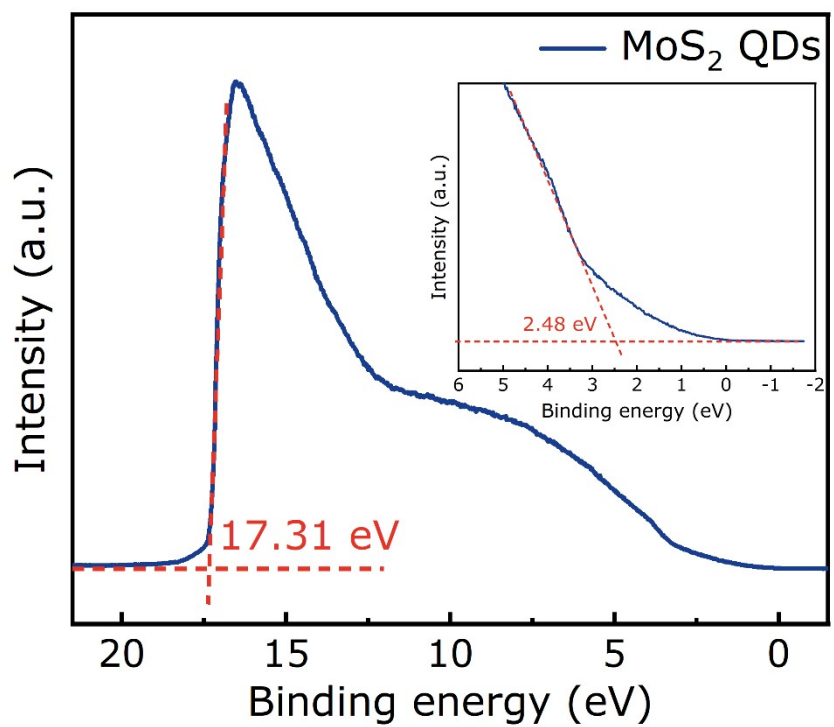


Fig. S13 Ultraviolet photoelectron spectra (UPS) of MoS_2 QDs.

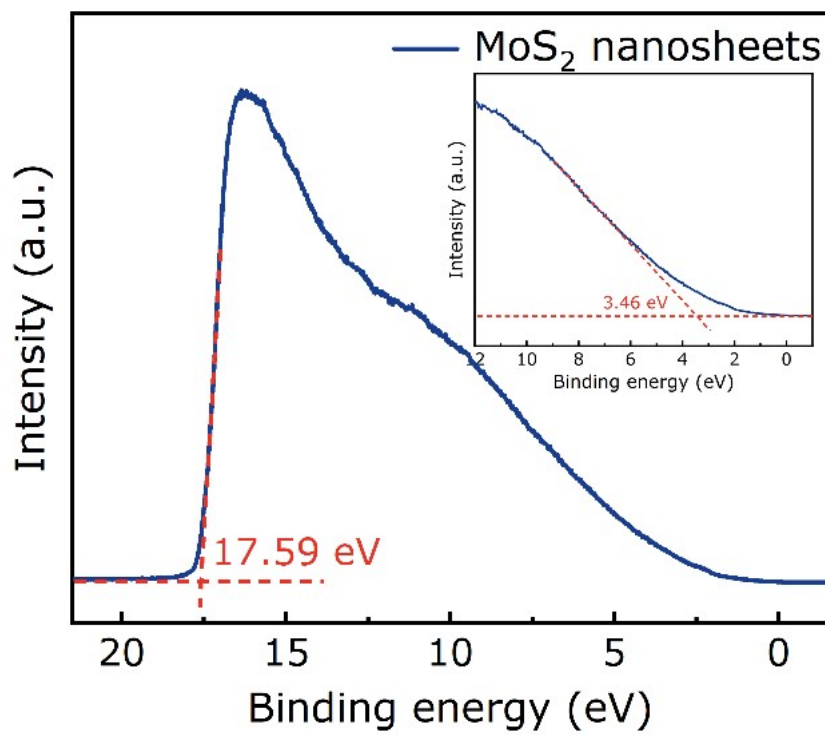


Fig. S14 Ultraviolet photoelectron spectra (UPS) of MoS_2 nanosheets.

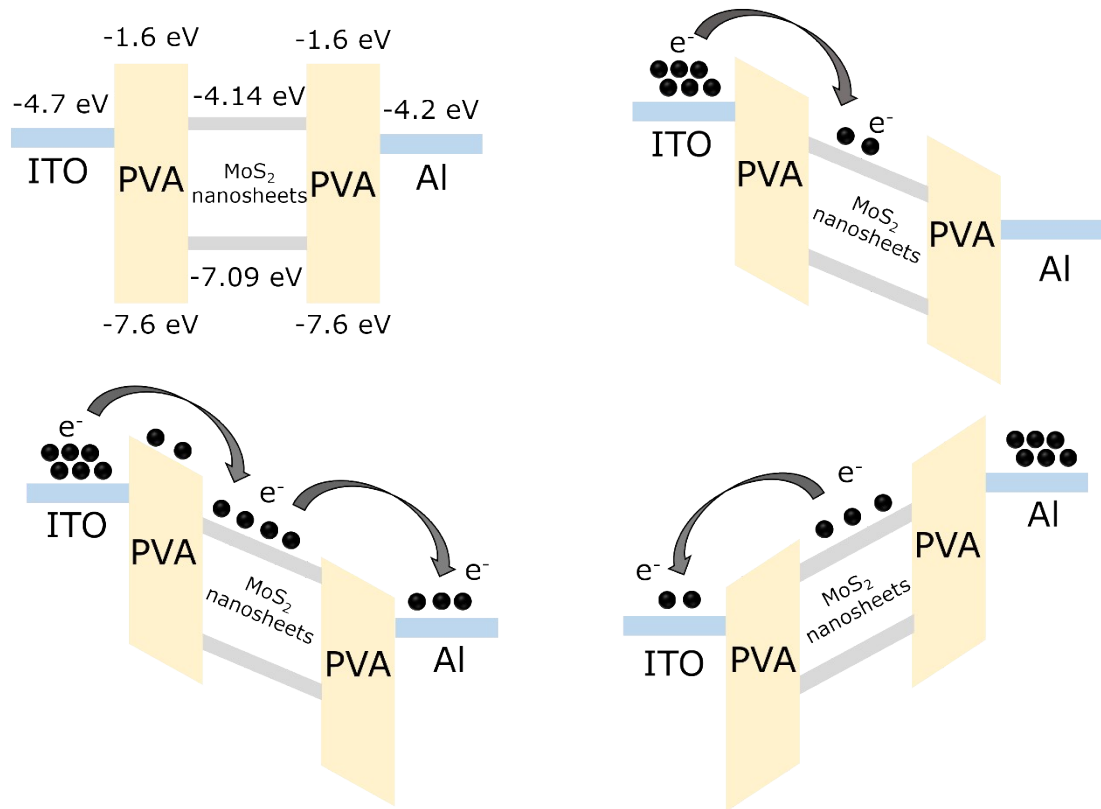


Fig. S15 Schematic diagram of the RS mechanism of Al/MoS₂ nanosheets-PVA/ITO/glass device.

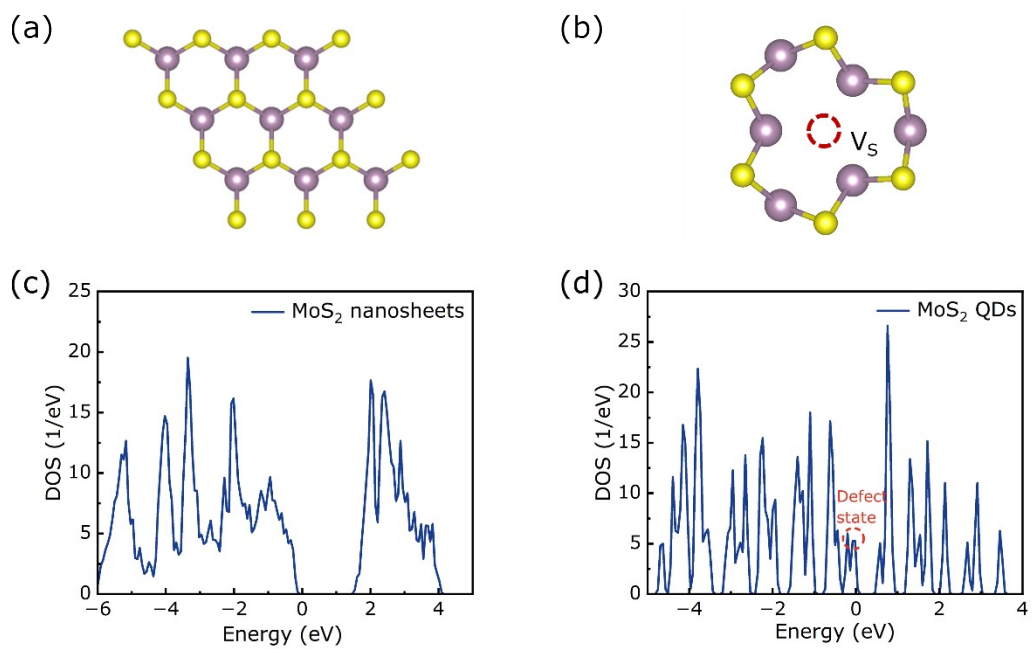


Fig. S16 Schematic diagram of crystal structure of (a) MoS₂ nanosheets and (b) MoS₂ QDs. The DOS plots of (c) MoS₂ nanosheets and (d) MoS₂ QDs.

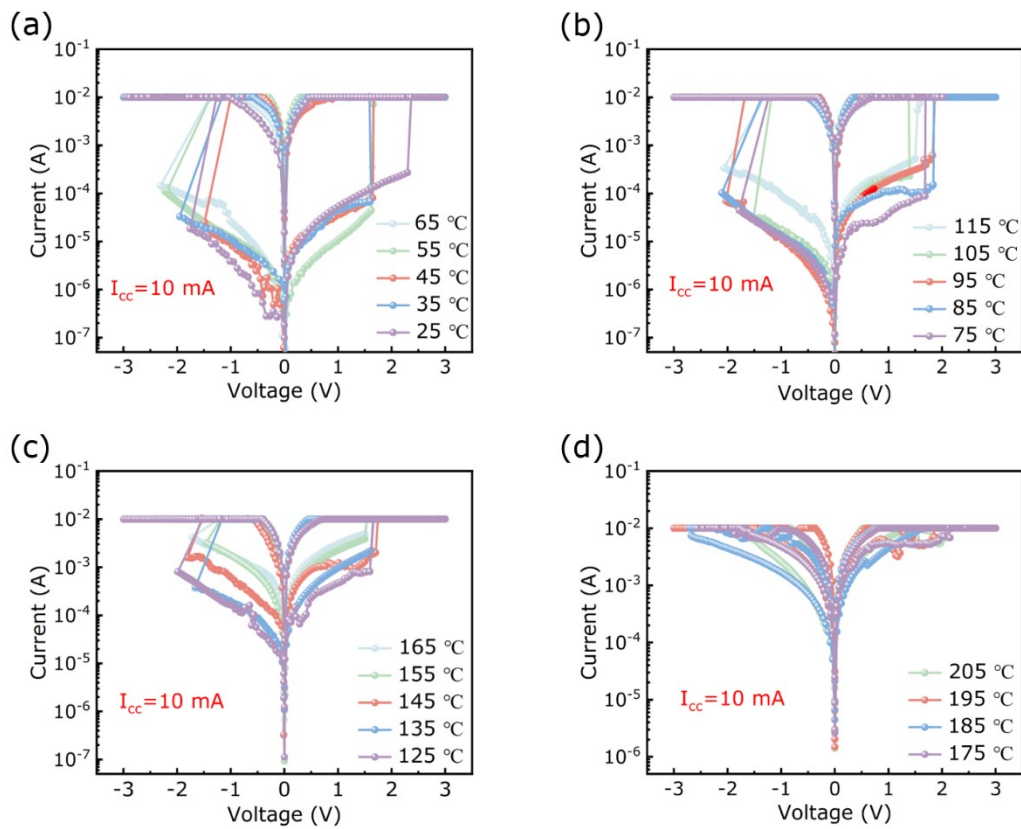


Fig. S17 2D plots of resistive switching corresponding to different temperatures for Al/MoS₂ QDs-PVA/ITO/glass device.

Tabel S2 Comparison of the key performance parameters of MoS₂-based RRAM device.

Structures	V _{reset} /V _{set} (V)	Endurance cycles	Retention time (s)	Referen ce
Al/MoS ₂ QDs-PVA/ITO/glass	-1.78/2.21	100	10 ⁴	This work
Al/MoS ₂ QDs/FTO	-1.35/2.2	30	10 ³	[3]
Au/MoS ₂ /Au	-0.9/2.7	20	10 ⁴	[4]
Ag/Ta ₂ O ₅ /MoS ₂ QDs/Pt	-0.1/0.2	200	10 ⁴	[5]
Au/MoS ₂ QDs/Au	-0.85/1.2	60	10 ³	[6]
ITO/(MoS ₂ :PS)/Al	-2.5/2.7	25	400	[7]
Al/CPB QDs/MoS ₂ /FTO/glass	-0.55/0.75	100	10 ⁴	[8]
Ag/MoS ₂ /Au/Ti/PET	-0.8/1.1	90	10 ⁴	[9]
ITO/QDs/MoS ₂ /TiO ₂ /Pt	-0.95/2.23	100	10 ⁴	[10]
Ag/ZnO/MoS ₂ QDs/W	-1.52/1.23	200	10 ⁴	[11]
Al/MoS ₂ -PDA-PFMMA/ITO	-0.9/1.1	60	10 ⁴	[12]

Reference

- 1 M. Saludes-Tapia, F. Campabadal, E. Miranda and M. B. González, *Solid-State Electronics*, 2023, **207**, 108718.
- 2 P. P. Patil, S. S. Kundale, S. V. Patil, S. S. Sutar, J. Bae, S. J. Kadam, K. V. More, P. B. Patil, R. K. Kamat, S. Lee and T. D. Dongale, *Small*, 2023, **19**, 2303862.
- 3 A. Thomas, A. N. Resmi, A. Ganguly and K. B. Jinesh, *Sci. Rep.*, 2020, **10**, 12450.
- 4 S. Bhattacharjee, E. Caruso, N. McEvoy, C. Ó Coileáin, K. O'Neill, L. Ansari, G. S. Duesberg, R. Nagle, K. Cherkaoui, F. Gity and P. K. Hurley, *ACS Appl. Mater. Interfaces*, 2020, **12**, 6022–6029.
- 5 X. Yu, K. Chang, A. Dong, Z. Gan, K. Jiang, Y. Ling, Y. Niu, D. Zheng, X. Dong, R. Wang, Y. Li, Z. Zhao, P. Bao, B. Liu, Y. Cao, S. Hu and H. Wang, *Applied Physics Letters*, 2021, **118**, 172104.
- 6 S. Sharma, Y. Chen, S. R. M. S. Santiago, S. A. Saavedra, C. Chou, K. Chiu and J. Shen, *Adv. Materials Inter.*, 2023, **10**, 2201537.
- 7 L. T. Manamel, S. C. Madam, S. Sagar and B. C. Das, *Nanotechnology*, 2021, **32**, 35LT02.
- 8 A. P. Deshmukh, K. Patil, S. Ogale and T. Bhave, *ACS Appl. Electron. Mater.*, 2023, **5**, 1536–1545.
- 9 R. M. Pallares, X. Su, S. H. Lim and N. T. K. Thanh, *J. Mater. Chem. C*, 2016, **4**, 53–61.
- 10 S.-Y. Tang, Y.-C. Shih, Y.-C. Shen, R.-H. Cyu, C.-T. Chen, T.-Y. Yang, M. Chaudhary, Y.-R. Peng, Y.-R. Kuo, W.-C. Miao, Y.-J. Yu, L. Lee, H.-C. Kuo and Y.-L. Chueh, *ACS Appl. Electron. Mater.*, 2024, **6**, 1581–1589.
- 11 Y. Li, X. Zhao, K. Chang, Y. Niu, X. Yu and H. Wang, *Phys. Rev. Applied*, 2022, **17**, 034007.
- 12 Q. Yan, F. Fan, B. Zhang, G. Liu and Y. Chen, *European Polymer Journal*, 2022, **174**, 111316.